

Ultrasonics International 83

Conference Proceedings



Ultrasonics International 83

Halifax, Canada 12-14 July 1983

Conference Proceedings

Conference organizer **Dr Z Novak**

Deputy organizer **S L Bailey**

Advisory panel

E E Aldridge, Prof. H O Berkay, Dr R C Chivers, I Flinn (dec'd), Prof. R E Green Jr, Dr R W G Haslett, Dr H W Jones (local organizer), Dr E A Neppiras, Dr R W B Stephens, Dr J Szilard, Dr P N T Wells

Butterworth Scientific Limited



Ultrasonics International 83

Hallifax, Canada 12-14 July 1983

Conference Proceedings

Published by Butterworth & Co (Publishers) Ltd, Borough Green, Sevenoaks, Kent, TN15 8PH

All rights reserved. No part of this publication may be reproduced, stored in a retrieval system or transmitted, in any form or by any means, electronic, mechanical, photocopying, recording or otherwise, without the permission of the publisher.

ISBN 0 408 22163 1

Printed in Great Britain

© 1983 Butterworth & Co (Publishers) Ltd

FOREWORD

The series of conferences, of which this is the fourteenth, began in 1964 under the title 'Ultrasonics for industry'. The programme then included eight papers presented over two days as an adjunct to the exhibition. Over the years the event has developed, with increasing numbers of presentations and overseas delegates. In 1979 it was held outside the United Kingdom for the first time, in Graz, Austria. This year a bigger leap was taken, across the Atlantic to Halifax, Nova Scotia to achieve an even wider international appeal.

This time 23 main sessions were presented together with two poster sessions. A wide variety of subject areas were covered - non-destructive testing, high power, medical and underwater ultrasonics, etc - reflecting the many different fields where ultrasound is playing an increasingly important role today.

With this volume the poster session papers are presented in full for the first time, reflecting the importance of their contribution to the programme.

This year another innovation was the panel discussion on 'Ultrasonics - trends for the future', which concluded the conference. I found this of great interest personally and I hope that you will share my opinion from the transcript published here. Indeed, I hope you find much of interest to you throughout the whole volume.

Dr Zdenek Novak
Conference Organizer
September 1983

Contents

Foreword

Session 1 Plenary session

- 1.1 Applications of ultrasonics in aerospace (abstract only) *J S Heyman* 1

Session 2 Non-destructive testing – 1

- 2.1 The defect sizing and characterization performance of an automated, multiprobe time-of-flight scanner *V S Crocker and G J Curtis* 2
- 2.2 Automatic in-motion inspection of the tread of railway wheels by EMA excited Rayleigh waves *H J Salzburger and W Repplinger* 8
- 2.3 The effect of material deformation on the velocity of critically refracted shear waves in railroad rail *D E Bray and M Najm* 13
- 2.4 Crack depth estimation using wideband laser generated surface acoustic waves *A M Aindow, J A Cooper, R J Dewhurst and S B Palmer* 20

Session 3 Medical ultrasonics – 1

- 3.1 Reflectivity tomography in attenuating media *J M Blackledge, M A Fiddy, S Leeman and D Seggie* 25
- 3.2 Mapping of internal material temperature with ultrasonic computed tomography *F Peyrin, C Odet, P Fleischmann and M Perdrix* 31
- 3.3 Wave propagation in biological tissue *R C Chivers and J D Aindow* 37
- 3.4 Ultrasonic Doppler measurement of blood flow volume rate in the abdomen *S E A Cole, M Qamar, M I Aldoori, R Skidmore, A E Read and P N T Wells* 43

Session 4 Acoustic emission – 1

- 4.1 A theoretical model for evaluating acoustic emission energy release during phase transitions of a shape-memory alloy *R S Geng, R G B Britton and R W B Stephens* 48
- 4.2 Acoustic emission in non-ceramic insulators *J Lanteigne* 54
- 4.3 Acoustic emission during martensitic transformation of iron-chromium alloy *H C Kim, J K Lee and S S Yu* 60
- 4.4 Acoustic emission during deformation and fracture of ceramics *G A Gogotsi, A V Drozdov and A N Negovskii* 67

Session 5 Visualization

- 5.1 A new stroboscope for schlieren and photoelastic visualization of ultrasound *G P P Gunaratne and J Szilard* 74
- 5.2 Digital ultrasonic imaging and its application to skeletal tissues *L Biro, P Das, A Meunier and J L Katz* 79
- 5.3 Acoustic imaging of cylindrical space *P Greguss* 85

Session 6 Material characterization

- 6.1 Ultrasonic characterization of oxygen contaminated titanium 6211 plate *S R Buxbaum and R E Green Jr* 91
- 6.2 Ultrasonic materials characterization of melt spun metallic ribbons *C L Friant and M Rosen* 97
- 6.3 Measurement of near-surface ultrasonic absorption by the thermoemissivity and application to the determination of the absorption in magnetic materials (abstract only) *J-P Monchalin and J Bussiere* 103

Session 7 Opto-acoustics – 1

- 7.1 On the crossroads of ultrasonics and optics
P Greguss 104
- 7.2 Experimental verification of diffraction of light by phase shifted adjacent ultrasound beams of frequency ratio 1: n , $n \gg 1$
P Kwiek, O Leroy, A Markiewicz and A Sliwinski 110
- 7.3 Optical absorption of powders determined by the photoacoustic effect
A B Rajab and R W B Stephens 116

Session 8 Non-destructive testing – 2

- 8.1 Computerized, robotic ultrasonic C-scan system for inspection of aerospace structures (abstract only)
B B Djordjevic 120
- 8.2 The calibration of ultrasonic equipment for measuring tube wall thickness
H D Ratray 121
- 8.3 Development of ultrasonic methods for the non-destructive inspection of concrete
T N Clayton and W A Ellingson 127
- 8.4 The use of ultrasonics for visualizing components of the prototype fast reactor whilst immersed in sodium
J A McKnight, J R Fothergill, L M Barrett, J A Parker, P Willis and R F Gould 135

Session 9 Physics of ultrasonics – 1

- 9.1 Propagation of ultrasonic waves in inhomogeneous media (abstract only)
A Zarembowitch, B Nouilhas, R Gohier and F Michard 141
- 9.2 Piezoelectrics as phonon echo generating materials
R M Holt, J O Fossum and K Fosshem 142
- 9.3 Measurement of transverse acoustic impedance: liquid helium
M J Lea, P Fozooni and P W Retz 148

Session 10 High power ultrasonics – 1

- 10.1 Large amplitude characteristics of bolt-clamped Langevin type vibrator
E Mori, S Ueha and Y Tsuda 154
- 10.2 A high power ultrasonic system for material testing and material compaction (abstract only)
W Tradinik, P Trimmel, K Kromp, W Kromp, F P Prinz and K H Staffa 160
- 10.3 An experimental study of the mechanics of ultrasonic tube-bending
I N Ibrahim and D H Sansome 161
- 10.4 Studies on the ultrasonic vibration press of powder with a vibration die
J Tsujino, T Ueoka, Y Atsumi, S Aoki and J Yamamoto 170
- 10.5 Fatigue of structural materials at ultrasonic loading frequencies
V A Kuz'menko 176

Session 11 Underwater ultrasonics

- 11.1 An ultrasonic exploration technique for finding oil under Arctic sea ice
H W Jones and H W Kwan 182
- 11.2 Tracking and imaging of a sound source using a sinusoidal frequency modulated ultrasonic wave
T Koda, H Mitome and S Shibata 188
- 11.3 The sensitivity of fisheries acoustic survey data to certain equipment parameters (abstract only)
L M Dickie, R G Dowd and P R Boudreau 194
- 11.4 A high frequency multichannel subbottom profiler
D P Schmidt, J A Vogel and J A van Woeden 195

Session 12 Non-destructive testing – 3

- 12.1 Acoustic stress measurement in aluminium and steel considering differences in texture due to rolled plate thickness
R B Mignogna, A V Clark, B B Rath and C L Vold 201
- 12.2 Ultrasonic time intervalometer for quantitative studies of surface properties in solids
K M Jassby, R Aharon, A Aharoni and D Longman 207
- 12.3 Immersion coupled phased array for inspection of offshore structures
M Macecek, K Luscott and J C Soumagne 214
- 12.4 Ultrasonics in offshore inspection
P E Boileau 220

Session 13 Medical ultrasonics – 2

- 13.1 Loudness of airborne ultrasonic noise
J Herbertz 226
- 13.2 Precision thickness gauging using digitized rf waveforms
M Freese, E Callway and P Wong 232
- 13.3 Attenuation estimation by spectral smoothing
L Hutchins and S Leeman 236
- 13.4 A diaphragm type strain gauge ultrasonic power meter
V N Bindal, V R Singh and R Gupta 242

Session 14 Physics of ultrasonics – 2

- 14.1 The nonlinear response of gas-filled micropores to ultrasound at MHz frequencies
E A Neppiras, W L Nyborg and D L Miller 248
- 14.2 Backscattering of a bounded ultrasonic beam at Rayleigh angle from plane and curved liquid-solid interfaces
M de Billy, G Quentin and L Adler 254
- 14.3 Parametric interaction of acoustic waves in a thermopiezosemiconducting medium
R K Pal, M Gupta and D K Sinha 259

Session 15 Acoustic microscopy

- 15.1 Acoustic microscopy: a new tool for the study of condensed matter
M Poirer and J D N Cheeke 265
- 15.2 A precision acoustic microscope for surface characterization
R D Weglein, R F Wilson and B W Maxfield 270
- 15.3 Acoustic microscope with Rayleigh angle incidence
C K Jen, G W Farnell and J C Soumagne 276

Session 16 Optoacoustics – 2

- 16.1 On the diffraction of light by adjacent parallel ultrasonic waves. A general theory
R Mertens and W Hereman 282
- 16.2 Optical generation of surface acoustic waves for photoacoustic microscopy and spectroscopy
G Veith 289

Session 17 Transducers – 1

- 17.1 New advances in the generation of directional sonic and ultrasonic radiation
J A Gallego, G Rodriguez, F Montero, E Andrés and J L San Emeterio 295
- 17.2 Temperature distribution in an ultrasonic power transducer
F B Stulen, N Senapati and R Gould 301
- 17.3 Field structures of disc transducers with specialized electrode configurations
D A Hutchins 307
- 17.4 Cyclic strength of piezoelectric ceramics for transducers
G G Pisarenko, V M Chushko and S P Kovalev 313

Session 18 Acoustic emission – 2

- 18.1 Comparison of simulated acoustic emission sources
M P Jones and R E Green Jr 319

18.2	Particle characterization by acoustic emission analysis <i>G A Rubin and M F Leach</i>	324
18.3	Acoustic emission linear pulse holography <i>H D Collins</i>	328
18.4	Acoustic emission study of electromigration induced extrusions in thin film Al/Cu conductors <i>H H Huston, E T Severn, J R Lloyd and G S Hopper</i>	333
Session 19 High power ultrasonics – 2		
19.1	Nonlinear acoustics: ancient foundations – modern objectives – exciting applications <i>L Bjørnø</i>	338
19.2	Studies on the ring type magnetic ultrasonic vibration detector <i>J Tsujino</i>	346
19.3	Ultrasonics for inhibiting biofouling <i>R J Taylor, L B Richardson and D T Burton</i>	352
19.4	Studies on ultrasonic metal welding – on the limit of ultrasonic spot welding and on the trial of ultrasonic butt welding <i>J Tsujino, T Ueoka and M Oyaide</i>	358
19.5	Recent advances in ink jet technology <i>J G Martner</i>	364
Session 20 Non-destructive testing – 4		
20.1	An ultrasonic signal analyser for automatic inspection of turbine discs <i>D I Crecraft</i>	373
20.2	Applications of controlled signals in ultrasonic testing of materials <i>H-A Crostack, W Oppermann and H Morlo</i>	379
20.3	Far-field signals from axis-symmetric sources in elastic plates <i>P-N Hsieh and W Sachse</i>	388
20.4	Defect discrimination using an ultrasonic echo phase method (abstract only) <i>S Sugiyama and S Ogura</i>	395
Session 21 Transducers – 2		
21.1	An under liquid electromagnetic acoustic transducer <i>R D Watkins, A B Gillespie, M O Deighton and R B Pike</i>	396
21.2	Theoretical and experimental study of the efficiency of an ultrasonic transducer <i>F Lakestani, J C Baboux, Y Jayet and M Perdrix</i>	402
21.3	Cardioid directivity conditions for a hydrophone <i>A Defebvre, J Pouliquen and J P Deparis</i>	408
21.4	Simulation of the acousto-electric response of ultrasonic narrow strip transducers with mechanical losses <i>R H Coursant, C Méquio and P Pesqué</i>	414
Session 22 Instrumentation		
22.2	A Fourier transform technique for the accurate measurement of phase delay of ultrasonic waves for residual stress determination <i>D R Allen and W H B Cooper</i>	420
22.3	Wideband spectral analysis of composite materials <i>H R Carleton and H Austerlitz</i>	426
22.4	Automated ultrasonic inspection and data collection system <i>J R Matthews, D R Hay and R W Y Chan</i>	432
Session 23 Physics of ultrasonics – 3		
23.1	Acoustic field analysis of SAW beams parametrically generated in nonlinear mixing processes <i>A Alippi, A Palma, F Palma, L Palmieri, G Socino and E Verona</i>	439
23.2	Surface and bulk waves interaction with periodic structures <i>A Jungman, G Quentin and L Adler</i>	446

23.3	Ultrasonic elastic wave model studies <i>L J Bond and R J Blake</i>	452
23.4	Ultrasonic testing of anisotropic media <i>M Brissaud and H Kleimann</i>	458

Poster sessions

1	A new non-invasive technique for detecting the presence of liquid at a specific level in a vessel <i>R D Watkins, A B Gillespie, M O Deighton and R B Pike</i>	464
2	Leak detection in recovery boilers using acoustic emission <i>D B Pape, F B Stulen and J D Maloney</i>	469
3	A high resolution relative ranging system using demodulated signal of sinusoidal fm ultrasonic wave <i>H Mitome, T Koda and A Shibata</i>	475
4	Impedance profiling of human tissues <i>S Leeman, J P Jones, J M Blackledge and D Seggie</i>	481
5	Photoelastic visualization of ultrasonic waves in a rail <i>A le Brun and J C Albert</i>	486
6	Orientation and structure of rf sputtered zinc oxide films on metal substrates <i>A S Khan and A Ambardar</i>	491
7	Shortening and standardizing the pulse shape of piezoelectric transducers in the megahertz region <i>C Hullin, H Rieder and H-J Welsch</i>	497
8	Polymerization initiated by ultrasonic cavitation <i>L A Dupont, P Kruus and T J Patraboy</i>	502
9	Studies of stress and creep relaxation under ultrasonic cyclic loading <i>Y I Tsimbalistyj and V I Vlasenko</i>	507
10	Ultrasonic propagation in plastically deformed sandstone (abstract only) <i>R M Holt and R K Bratli</i>	513
11	A selective audio signalling system <i>V N Bindal, T K Saksena and M Chandra</i>	514
12	Localized hyperthermia by ultrasound and its repartition <i>O Prakash, M L Gaulard and A Tosser</i>	519
13	Computer control of radiated pressure from an ultrasonic projector <i>J D Birdwell, Y-C Jin, T J Paulus, C J Mazzola and R W Barnes</i>	524
	Panel discussion 'Ultrasonics – trends for the future'	531
	Author index	539

J S Heyman

Materials Characterization Instrumentation Section, NASA-Langley Research Center,
Hampton, Virginia, USA

Lighter, stiffer, hotter, colder, more reliable and longer life are typical demands placed on aerospace structures and elements. The rapid growth of technology in that field has presented many opportunities and challenges for nondestructive evaluation (NDE). As rapidly as new materials appear, the need exists for NDE applied to that material. These requirements have resulted in many advances from flaw detection/evaluation to actual materials characterization. In this review, we shall present two recent advances based on physical acoustics and briefly discuss several others. The first involves use of ultrasonics to characterize changes in stress in structural elements and the second involves a phase insensitive ultrasonic transducer for quantitative analysis of a most significant aerospace material-composite.

A simple structural element that most people take for granted is the critical fastener. In aircraft as well as spacecraft applications, proper bolt preload is necessary for structural performance. A variety of frictional errors reduce the accuracy of torquing systems to an unacceptable level for some applications. However, ultrasonic natural velocity measurements are insensitive to friction and permit accurate measurements of stress changes directly in the fastener. Examples of several critical fasteners and ultrasonic data obtained with them will be presented.

A second and unusual challenge for NDE is presented by lightweight fiber stiffened composite materials. The materials are inhomogeneous, geometrically irregular, anisotropic, highly absorptive and sensitive to impact. An ultrasonic plane wave incident normally to such a material is certainly neither plane nor normal after an appreciable propagation path. The complexities of correct attenuation measurements in composite materials stem in part from the phase sensitive nature of conventional transducers. Examples of phase cancellation in typical measurements will be presented and compared to data obtained with a phase insensitive power detector. A significant reduction in measurement error is shown for a variety of examinations in inhomogeneous/irregular materials that have important functions in aerospace applications.

Additional topics to be briefly discussed include a fiber optic acoustic emission sensor and "scale up" problem necessary to test hardware on the Space Shuttle.

(1)

$$T = \frac{2}{c} \sqrt{L^2 + d^2}$$

where d = vertical depth of the crack top/bottom beneath the surface,
 $2L$ = spacing between the points of entry and exit of the pulse in the surface,
 c = velocity of compressional waves in the metal.

THE DEFECT SIZING AND CHARACTERISATION PERFORMANCE OF AN AUTOMATED, MULTIPROBE TIME-OF-FLIGHT SCANNER

V S Crocker and G J Curtis

United Kingdom Atomic Energy Authority, Atomic Energy Research Establishment,
Harwell, Didcot, England.

During 1981/82 a round robin exercise (The Defect Detection Trials) took place to assess the capability of a number of ultrasonic techniques being used in Europe. The Trials used a range of simulated PWR pressure vessel sections. A Harwell contribution to these Trials was the deployment of a computer controlled, multi-probe ultrasonic time-of-flight system. This technique in its simple form had hitherto been considered as an accurate defect sizing technique. The Trials revealed that the technique can also be used to detect defects and to characterise them. This paper illustrates the progress made in characterising planar, fatigue and branched cracks.

INTRODUCTION

During the period May 1980 to December 1981 the United Kingdom Atomic Energy Authority carried out a round robin exercise¹ (The Defect Detection Trials) to assess the defect location and sizing capability of a number of ultrasonic techniques currently being practised in Europe. The trials used a range of test samples which closely simulated sections of a PWR pressure vessel. One of the Harwell contributions to these Trials was to deploy a minicomputer controlled, multiprobe, technique based upon the two probe time-of-flight technique (TOFT) developed by Silk^{2,3} and his co-workers. In this, crack detection is by observation of the forward scatter of ultrasound from the top and/or bottom of a crack and crack-through-thickness sizing by timing the flight of a pulse from the transmitter probe down to the crack and thence up to the receiver. Currently a detailed destructive examination is being made of the various types of defects inserted into the Trial welds. Initial data obtained shows that the Harwell TOFT technique performed well in both defect location and sizing. The data also indicates that the technique has potential in characterising the morphology of a defect, and initial results in this field are reported.

ACOUSTIC DESIGN FOR THE MULTIPROBE SCANNER

In Silk's two probe arrangement (described in detail elsewhere²) when the sender and receiver symmetrically straddle a crack, the time-of-flight T , of a compressional wave as it travels in the solid down to the crack and scatters up to the surface again may be expressed as follows:-

$$T = \frac{2}{c} (L^2 + d^2)^{\frac{1}{2}} \quad (1)$$

where d = vertical depth of the crack top/bottom beneath the surface,
 $2L$ = spacing between the points of entry and exit of the pulse in the surface,
 c = velocity of compressional waves in the metal.

The depth of the crack, d , could thus be determined by observing T for a chosen value of L and a knowledge of c . In practice it is useful to make use of that part of the refracted beam which is critically internally refracted. This arrives at the receiver first and can be used as a timing reference. (As will be discussed later it disappears if a surface breaking crack is between the probes, otherwise its continued presence indicates that there is no transmitter or receiver malfunction). If t is the time difference between the arrival of the critically internally refracted lateral wave pulse and the pulse from the crack, it can be shown that the accuracy in measuring t , ie δt , relates to the accuracy of depth assessment δd by:-

$$\delta d = \frac{c}{2 \cos \theta} \delta t \quad (2)$$

where θ = the angle of refraction chosen.

Using a 20MHz digitiser to convert the ultrasonic signal for digital processing, a basic error in t of one sampling interval, $0.05 \mu\text{sec}$, might be expected. In a steel where $c = 5900 \text{msec}^{-1}$

$$\delta d = \frac{0.15 \text{mm}}{2 \cos \theta} \quad (3)$$

This indicates that to achieve an accuracy of depth measurement of $\pm 1 \text{mm}$ the angle θ needs to be less than 80° .

Given that θ should be less than 80° , it is desirable to choose θ to yield the largest forward scattered signal at the receiver. Temple⁴ suggests that the angular dependence of the signal amplitude shows a principal peak at 65° . Silk's³ experimental evidence is for a peak at $\theta \sim 60^\circ$. In the design of the scanner the useful refraction range was considered to be $60^\circ \pm 20^\circ$.

The American Society of Mechanical Engineers Code of Practice XI calls for inspection of not only the weld cross section, but also the parent plate for a distance of half the through-thickness on either side of the weld walls. This, together with the desirable angle-of-refraction set by the demand for strongest signal and a measurement accuracy of $\pm 1 \text{mm}$, provides the basic constraints upon the acoustic design for the scanning head. Ray tracing then shows that it is possible to cover the required cross-section with the useful part of the beams of an array of 8 transmitting and 8 receiving probes. With such a fixed array it is possible simply to straddle the weld and move linearly along it gathering ultrasonic data from chosen transmitter-receiver pairs by computer control. One linear traverse is sufficient to inspect the ASME XI coded weld volume. Fig. 1 shows the scanning head which was constructed to inspect the 250mm thick ferritic butt-welds clad with $\sim 10 \text{mm}$ of austenitic cladding. The transducers are Aerotek alpha series probes with a centre frequency of 5MHz and diameters of 10mm for near surface inspection and 25mm for inspection of the lower weld regions. First stage amplifiers are also mounted on the head.

The scanning operation and collection of data is carried out by an on-line HP1000 minicomputer. Up to 64 combinations of probes can be addressed, but in practice 40 combinations are found sufficient. Using the digitisation rate of 20MHz, A-scan data is accumulated onto magnetic tape. The duration of a scan depends upon the amount of averaging desired. (For the outermost probes this may be 100 pulses, whereas none is required for the closely spaced probes). Typically the scan speed is 1.6mm per minute.

DATA ANALYSIS FOR THE MULTIPROBE SCANNER

Data analysis is carried out on a PDP11/60 minicomputer complemented by a Stanford Technology I²s(70E) frame store display. Using this, B-scan views of the longitudinal-thickness plane of the weld can be presented on an interactive graphics

monitor for any of the transmitter-receiver combinations which were recorded. The raw, distance-time domain of a typical B-scan is commonly distorted due to the surface undulations of the clad specimen. Depth determinations are thus carried out from a processed B-scan where the lateral wave signal is rendered flat. Interactive graphics programming provides the operator with a cursor superimposed upon the B-scan, which he can move to any feature to determine its location. By pressing a button the location coordinates are displayed on an associated VDU. Accurate determination of depth is done by processing depth measurements from a number of transmitter-receiver combinations (typically 10). To make a determination of the length of a defect in the weld direction (ie scan direction) the B-scan is further processed, this time by synthetic aperture processing, SAFT, to yield a distance-distance domain view which is not impaired by beam spreading⁵. Fig. 2 shows a typical TOFT + SAFT view for an interface breaking fatigue crack.

DEFECT SIZING ACCURACY ACHIEVED WITH THE MULTIPROBE SCANNER

The Defect Detection Trials provided an opportunity to establish the detection and sizing capability of the Time-of-Flight technique in a blind test on 250mm thick welds clad with 10mm austenitic steel, containing defects which closely simulate those which could occur in practice, albeit with a very low probability, in a PWR vessel. Correlation with the destructive data obtained so far suggests that the technique is not only capable of detecting defects, but has an accuracy in determining the critical through-thickness dimension of a defect of $\pm 1.5\text{mm}$.

DEFECT CHARACTERISATION WITH THE MULTIPROBE SCANNER

The defect types included in the Defect Detection Trial specimen weld number 2 were: lack-of-wall fusion, lack-of-root fusion, fatigue cracking, planar cracking, branched cracking and slag entrainment. These provided an opportunity to examine the defect characterisation potential of the Time-of-Flight Technique. (A full destructive examination has yet to be completed, however initial data from detailed C-scans on partially sectioned material, yields data for an initial correlation). Since TOFT relies upon imaging forward scattered and specularly reflected energy from appropriately oriented facets of a defect, it is capable of showing-up considerable detail in the defect. Using a short pulse of 5MHz centre frequency, together with SAFT processing, achieves this capability. Facets of the defect which lie parallel to the surface are most strongly defined, whereas facets which lie normal to the surface are undefined.

The scope of this paper does not allow a detailed presentation of the images obtained for all the defect types studied (this will be done elsewhere⁶) it does however, allow presentation of three types of defect:

(a) An interface breaking fatigue crack

Fig. 2a shows the TOFT and SAFT view. It will be seen that the interfacial wave (lateral wave) is broken indicating that the top of the defect lies close to the cladding-ferritic interface. Scatter from the bottom of the crack is strong and the bottom appears stepped. (Two satellite, unintentional welding defects are also imaged near to the bottom, C and D). Analysis with probe combination which yielded this figure together with all others which were oriented to view the defect, produced the drawing of the defect shown in Fig. 2b. The broken line indicates the latest data obtained from the destructive examination, which includes detailed local C-scanning. The full line indicates the data obtained from TOFT + SAFT. The correlation in sizing is clearly very good, and the suggestion of an stepped bottom to the defect is justified.

(b) A buried, branched crack

As a contrast to Fig. 2a, Fig. 3a shows the TOFT + SAFT view of a buried branched

crack. It appears as a complex array of isolated scattering elements. The technique does not, as it currently stands, allow a description of how these elements might be interconnected. This view, plus those for other probe combinations, does facilitate the drawing of the defect as shown in Fig. 3b. The facets are depicted as isolated spots. Superimposed upon this is the currently available detailed C-scan view from the destructive examination. The latter suggests an irregular area for the defect. When detailed sectioning is carried out it may be possible to establish a closer spatial correlation. (Work on other similarly produced defects anticipates branched cracking). As it is now, the correlation is more than adequate for inspection sizing purposes. If the defect is found to be an array of unconnected defects, then TOFT + SAFT characterisation will be a very valuable addition.

(c) A buried, planar crack.

Fig. 4a shows the TOFT + SAFT view of a buried planar crack. It appears to have a stepped top and irregular bottom. By contrast with Fig. 3a it is simpler. The crack would not appear to be so fragmented. (This type of defect was induced by carbon contamination and is expected to be approximately planar). This view of the defect, plus those from other probe combinations, yields the drawing shown in Fig. 4b. The stepped top and irregular bottom is depicted with full lines. Superimposed upon it is the data currently available from the detailed C-scan view of the destructive examination, and it supports the view obtained from TOFT + SAFT

INITIAL CONCLUSIONS

The Defect Detection Trials have established that the Time-of-Flight Technique is capable of sizing the critical through-thickness dimension of a defect, however deep it may be in the 250mm cross section of a PWR girth weld, to an accuracy of $\pm 1.5\text{mm}$. This makes it probably the most precise sizing technique currently available. Such accuracy is comparatively simply achieved. Pre-prototype scanning devices have been engineered even for a complex geometry such as the inside surface of the PWR vessel where it is penetrated by the coolant nozzles.

Complete destructive examination of the DDT specimens has yet to be carried out. Initial data does, however, suggest a correlation emerging between the detailed spatial description of defects by TOFT and that being found destructively. As we have presented here, different defect morphologies do yield different TOFT + SAFT views and it is clear that the defect characterisation potential is worth active perusal.

REFERENCES

1. Watkins B: Results of the UKAEA Defect Detection Trials to be published by HMSO.
2. Silk M: "Defect sizing by ultrasonic diffraction" British J. NDT 21 (1), 12, 1979.
3. Silk M: Transfer of ultrasonic energy in the diffraction technique for crack sizing" Ultrasonics 17 (3), 113, 1979.
4. Temple A: "Time-of-flight inspection with compression waves: cracks and slag-lines" AERE T.P. Report 932, 1981.
5. Curtis, G.J.: "Ultrasonic synthetic aperture focussing" Proc. of the Symp. on Inspection of UK Reactors, BNES, Sept. 30, 1980.
6. Curtis, G.J.: To be published.

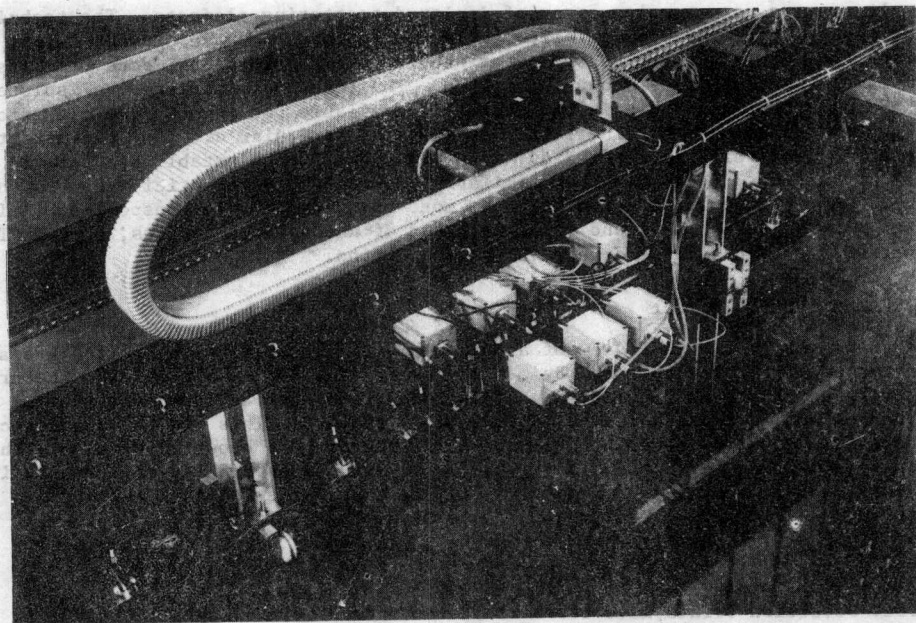


FIG. 1 FLAT PLATE SCANNING HEAD

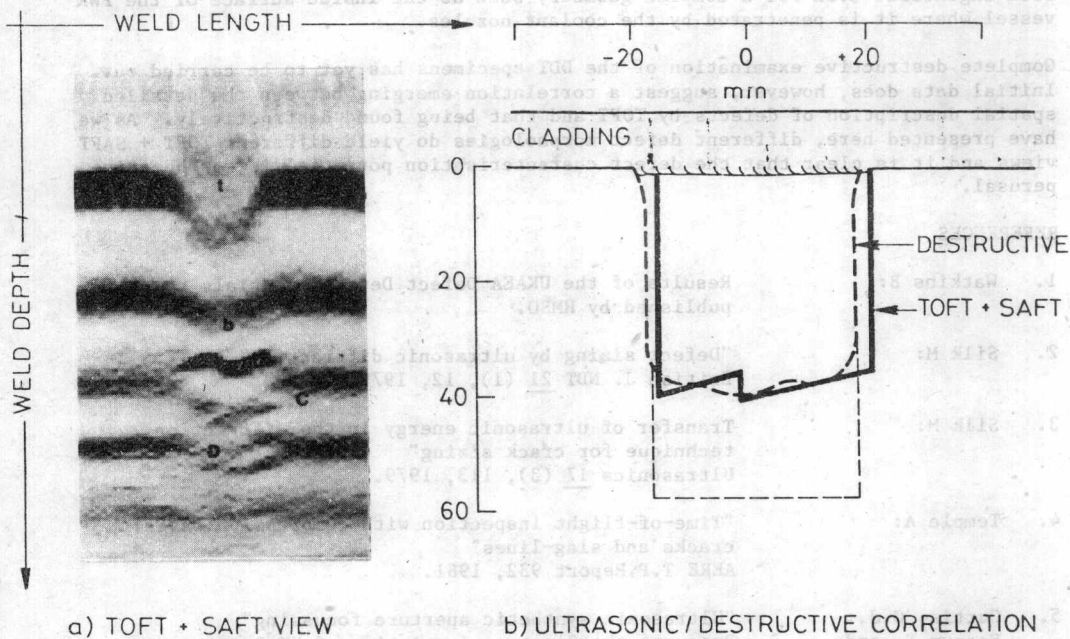
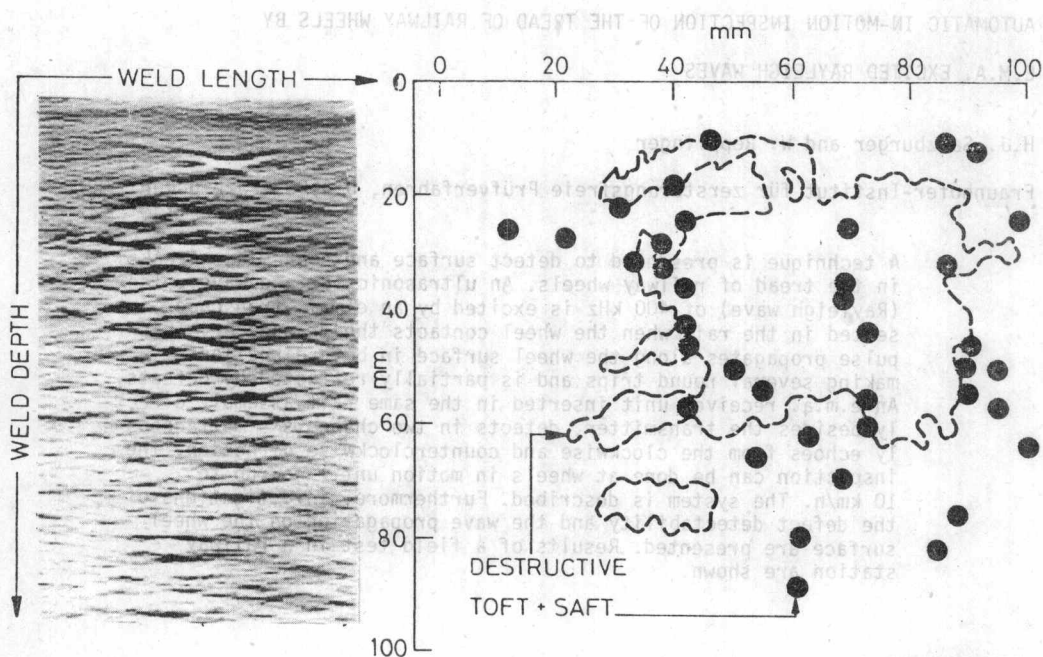


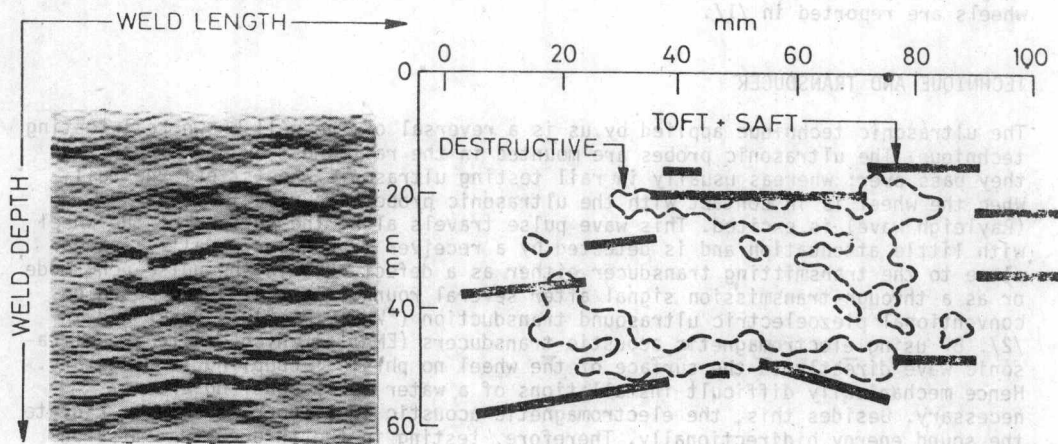
FIG. 2 TOFT + SAFT EXAMINATION OF A FATIGUE CRACK



a) TOFT + SAFT VIEW

b) TOFT + SAFT / DESTRUCTIVE CORRELATION

FIG. 3 TOFT + SAFT EXAMINATION OF A BRANCHED CRACK



a) TOFT + SAFT VIEW

b) TOFT + SAFT / DESTRUCTIVE CORRELATION

FIG. 4 TOFT + SAFT EXAMINATION OF A PLANAR CRACK

AUTOMATIC IN-MOTION INSPECTION OF THE TREAD OF RAILWAY WHEELS BY

E.M.A. EXCITED RAYLEIGH WAVES

H.J. Salzburger and W. Repplinger

Fraunhofer-Institut für zerstörungsfreie Prüfverfahren, D-6600 Saarbrücken, FRG

A technique is presented to detect surface and subsurface cracks in the tread of railway wheels. An ultrasonic surface wave pulse (Rayleigh wave) of 400 kHz is excited by an e.m.a. transducer inserted in the rail when the wheel contacts the transducer. This pulse propagates along the wheel surface in both directions making several round trips and is partially reflected by defects. An e.m.a. receiver unit inserted in the same rail assembly directly besides the transmitter, detects in two channels simultaneously echoes from the clockwise and counterclockwise direction. The inspection can be done at wheels in motion until now up to 10 km/h. The system is described. Furthermore, investigations of the defect detectability and the wave propagation on the wheel surface are presented. Results of a field test in a railway station are shown.

INTRODUCTION

In wheel-rail systems the undercarriage and especially the rim are exposed to high loads. By dynamic working conditions damages of the wheels occur such as cracks (thermal and fatigue cracks) or breaking of the tyre. There is no knowledge how these defects evolve. Their timely detection is instrumental in the enhancement of the safety.

Some of these defects can be verified by visual inspection. This is not possible for surface cracks in the tread of wheels that are peened over because of their long running time. Basic studies on the detectability of defects on model railway wheels are reported in /1/.

TECHNIQUE AND TRANSDUCER

The ultrasonic technique applied by us is a reversal of the well-known rail testing technique. The ultrasonic probes are mounted in the rail and they check wheels as they pass over; whereas usually in rail testing ultrasonic wheels test the rail. When the wheel is in contact with the ultrasonic probe, a surface wave pulse (Rayleigh wave) is excited. This wave pulse travels along the surface of the wheel with little attenuation and is detected by a receiver transducer usually located close to the transmitting transducer either as a defect echo in the pulse-echo mode or as a through-transmission signal after several round trips. A system based on conventional piezoelectric ultrasound transduction ("WHEEL FAX") is described in /2/. By using electromagnetic acoustic transducers (EMAT's) which excite the ultrasonic wave directly in the surface of the wheel no physical coupling is necessary. Hence mechanically difficult installations of a water spray coupling are not necessary. Besides this, the electromagnetic acoustic transducer is able to radiate the sound energy bidirectionally. Therefore, testing in the through-transmission and pulse-echo mode is simultaneously possible.

The EMAT inserted in the rail is schematically shown in Fig. 1. It consists of an electromagnet in the lower part of the recess of the rail which produces a magnetic field normal to the rail surface. The HF-coil which is a meanderlike coil is